International Journal of Food Microbiology 311 (2019) 108350

Contents lists available at ScienceDirect

International Journal of Food Microbiology

journal homepage: www.elsevier.com/locate/ijfoodmicro

Succession rate of microbial community causes flavor difference in strong-aroma *Baijiu* making process

Yuwei Tan[a,1], Heping Zhong[a,b,1], Dong Zhao[b], Hai Du[a,*], Yan Xu[a,*]

[a] Key Laboratory of Industrial Biotechnology of Ministry of Education, State Key Laboratory of Food Science and Technology, Synergetic Innovation Center of Food Safety and Nutrition, School of Biotechnology, Jiangnan University, 1800 Lihu Avenue, Wuxi, Jiangsu 214122, China
[b] Key Laboratory of Wuliangye-Flavor Liquor Solid-State Fermentation, China National Light Industry, Yibin, Sichuan, China

ARTICLE INFO

Keywords:
Microbial interaction
Cereals
Pit mud
Microbial source tracking
Solid-state fermentation (SSF)

ABSTRACT

Solid-state fermentation is a dynamic process involved with complex microbiome. Microbial structure and succession significantly affect the yield and quality of fermentation productions. Although the importance of microbial structure was extensively studied, the significance of microbial succession rate remains unclear in solid-state fermentation. To address this gap, we designed an in situ experiment in a typical distillery to characterize the effects of microbial succession rate. In this study, we found the process of strong-aroma *Baijiu* making could be divided into two stages according to fermentation parameters (starch, moisture, acidity, reducing sugar, alcohol, temperature). The early stage showed significantly ($p < 0.05$) higher microbial diversity than that of the later stage according to Shannon index. Compared with single cereal fermentation, mixed cereals fermentation showed slower microbial succession rate of stage shift. We found that *Lactobacillus* could reflect microbial succession rate of stage shift in strong-aroma *Baijiu* fermentation. Meanwhile, we found fermentation parameters could affect microbial succession rate of stage shift. Microbial diversity was significantly ($p < 0.05$) correlated with fermentation parameters. Moreover, molecular ecological network analysis (MENA) showed that succession rate of microbial community could affect microbial interactions. In addition, fermentation of mix cereals (sorghum, wheat, corn, rice and glutinous rice) increased the enrichment of Clostridiales from pit mud according to results of source tracking. Collectively, succession rate of microbial community could be an important trait to explain differences of microbial diversity and flavor profile from the perspective of microbial decline and enrichment. Our study highlighted the importance of microbial succession rate during strong-aroma *Baijiu* making process and provided a dynamic perspective to observe solid-state fermentation.

1. Introduction

Diverse combinations of raw materials and starter generate a variety of fermented products, such as wine, vinegar, cheese and *Baijiu* (Chinese liquor) in the long history. Complex microbial community can affect yield and quality of fermentation productions (Dunkel et al., 2014; Lu et al., 2018; McAuliffe et al., 2019). Spontaneous food fermentation can hardly be controlled without understanding the importance of microbial community. The relationship among microorganisms, raw materials and metabolites is a widely concerned scope in fermentation (Ai et al., 2019; Bokulich et al., 2016; Nie et al., 2017).

Baijiu, distilled from fermented grains, is a typical solid-state fermentation product. Although *Baijiu* can be produced by several combinations of cereals and starters (Hu et al., 2016; Jin et al., 2017), the yield and quality of products may differ from each other (Fan and Qian, 2006; Jin et al., 2017; Liu and Sun, 2018). To explain that, researchers studied fermentation differences from perspectives of raw materials (Du et al., 2019; Wu et al., 2017), porosity of the grains (Jiang et al., 2016), microbial diversity (Shi et al., 2011) and microbial transcription (Song et al., 2017) during *Baijiu* making process. However, only a few studies illustrated the fermentation process in a dynamic aspect. Meanwhile, the importance of microbial succession rate was rarely underlined in *Baijiu* making process.

Previous ecological study suggested that microbial succession rate could reflect the process of microbial assembly (Datta et al., 2016). Microbial succession rate is an important biological trait related to microbial fitness, microbial stability and microbial coexistence (Cira et al., 2018; Grainger et al., 2019). Besides, the community-level function is highly predictable governed by nutrient availability (Goldford et al., 2018). Observation and simulation of micro-ecological

* Corresponding authors.
E-mail addresses: duhai88@126.com (H. Du), yxu@jiangnan.edu.cn (Y. Xu).
[1] Both authors contributed equally to the manuscript.

https://doi.org/10.1016/j.ijfoodmicro.2019.108350
Received 17 May 2019; Received in revised form 4 September 2019; Accepted 5 September 2019
Available online 06 September 2019

systems can be helpful to discover microbial function and succession mechanisms (Layeghifard et al., 2017). Therefore, we designed an in situ fermentation experiment in a typical distillery (Fig. S1) to reveal the influence of microbial succession rate on the strong-aroma *Baijiu* making process of single cereal and mixed cereals fermentation.

In this study, volatile compounds were detected via a head space-solid phase micro-extraction combined with full two-dimensional gas chromatography-time of flight mass spectrometry (HS-SPME-GC × GC-TOFMS) to figure out fermentation difference between single cereal and mixed cereals fermentation. Illumina-based high-throughput sequencing method was conducted to investigate the microbiota dynamics during the fermentation processes. Furthermore, the Shannon index was calculated to describe microbial diversity across fermentation process. In addition, fermentation parameters (starch, moisture, acidity, reducing sugar, alcohol, temperature) were determined to analyze the driving force of microbial succession.

2. Material and methods

2.1. Experimental design and sample collection

The experiment was carried out at a well-known strong aroma distillery (Wuliangye Co. Ltd.) in Yibin City, Sichuan Province, China. Three batches of fermentation were executed in rectangular-shaped pits (2 m × 3 m × 2 m) underground, named group S, group T and group F (Fig. S1). Each batch of pit fermentation used different raw materials, but the same *Daqu* (starter). Group S used sorghum as the raw material of fermentation. Group T used sorghum, corn and wheat as the raw material of fermentation. Group F used sorghum, corn, wheat, rice and glutinous rice as the raw material of fermentation.

After 58 days of pit fermentation, we started the distillation of fermented grains. The base liquors were collected from condensate pipe for further analysis. In addition, we collected fermented grains samples at 4, 7, 9, 13, 19, 25, 31, 40, 49, 58 days after fermentation in each batch. Furthermore, 15 upper (N1, N2, N3, N4, N5, N6, N7) and middle (ZN1, ZN2, ZN3, ZN4, ZN5, ZN6, ZN7, ZN8) layers of pit mud and one *Daqu* (Q1) were sampled. All starter samples were mixed before detection. Hence, we totally collected one samples of starter, 15 samples of pit mud, 3 samples of base liquor and 30 samples of fermented grains.

2.2. Volatile compounds analysis

In order to ensure the representativeness of experimental design and clarify the main volatile metabolites difference between groups, we collected the base liquor and its corresponding fermented grains before distillation in each group.

The volatile compounds of fermented grains were extracted by HS-SPME (Divinylbenzene/Carboxen/Polydimethylsiloxane) and analyzed by GC–MS (GC 6890N, MS 5975, Agilent Technologies, Santa Clara, CA). Samples was treated as following details: 5 g fermented grains were diluted 4 times by 20 ml sterile saline (1% $CaCl_2$, 0.85% NaCl) in 50 ml centrifuge tubes, then ultrasonically treated in ice-bath after full oscillation. After that, the sonicated samples were centrifuged at 4 °C, 1000 ×*g* for 5 min. We pipetted 8 ml supernatant into a headspace bottle with 3 g NaCl, adding 10 μl menthol as the internal standard (106.25 ppm), then carry on the HS-SPME-GC–MS (column: DB-Wax, 30 m × 0.25 mm × 0.25 μm) according to the method described by Gao et al. (2014).

The volatile compounds of base liquors were analyzed via HS-SPME-GC × GC-TOFMS based on the method described by Yao et al. (2015). Every base liquor (800 μl) was diluted 10 times by ultra-pure water in the headspace bottle with 3 g NaCl before detection. To avoid overload of detector, the peak of ethanol was neglected via adjusting signal collection according to retention time. After detection, the peaks with matching similarity > 70.00% were screened and normalized.

2.3. Fermentation parameters detection and analysis

To understand the fermentation processes of mixed cereals and single cereal fermentation, we analyzed six fermentation parameters, including starch, reducing sugar, acidity, alcohol, moisture and temperature, to figure out features of fermentation stages. The moisture of fermented grains was determined by a gravimetric method by drying samples to a constant weight at 105 °C for at least 3 h. The alcohol content of fermented grains was determined via alcoholmeter after distillation. The total titratable acidity of fermented grains was determined by titration with NaOH (0.1 M), indicated through phenolphthalein (end-point of pH 8.2). The contents of total starch and sugar were monitored by the method described by Bravo et al. (Bravo et al., 1998) and Miller et al. (Miller, 1959). The temperature of fermented grains was determined via button thermometer. Bray-Curtis dissimilarity matrix of fermentation parameters was calculated to generate a principal coordinate analysis (PCoA) plot.

2.4. Total DNA extraction, amplification and Illumina MiSeq sequencing

Total DNA was isolated using the EZNA™ (Easy Nucleic Acid Isolation) Soil DNA Kit (Omega bio-tek; Norcross, GA) according to the manufacturer protocol. For bacteria, V3-V4 hypervariable region of the 16S rRNA gene was amplified using the primer sets F338 and barcode R806. For fungi, the internal transcribed spacer (ITS) region was amplified with primers ITS1F and ITS2R. PCR products were purified by a PCR purification kit, the concentrations were carefully assessed by Thermo Scientific NanoDrop 8000 UV–Vis Spectrophotometer (NanoDrop Technologies, Wilmington, DE). The barcoded PCR products were sequenced on a Miseq Benchtop Sequencer for 250 bp pair-end sequencing (2 by 250 bp; Illumina, San Diego, CA) in Beijing Auwigene Tech. Ltd. (Beijing, China).

2.5. Processing of sequencing raw data

Raw sequences were processed by Qiime (v1.8.0) (Caporaso et al., 2010). Briefly, the raw sequences were quality-filtered, and sequences with ambiguous bases ('N') were removed by Trimmomatic (version 0.32) (Bolger et al., 2014). Chimera sequences were removed using the Uchime algorithm (Edgar et al., 2011). The high quality sequences were clustered (97% sequence similarity) into OTUs using Qiime's Uparse pipeline. In addition, OTUs of 16S rRNA gene amplicons were mapped to Silva (version 128) (Zhang et al., 2015) and OTUs of ITS amplicons were mapped to Unite (version 7.0) (Kõljalg et al., 2013). Then alpha biodiversity was analyzed via Qiime.

2.6. Data processing and visualization of volatile compounds

The peaks with matching similarity > 70% were screened, and the area percentage of each peak were calculated according to relative signal intensity. The O/C ratio versus H/C ratio was calculated based on each assigned monoisotopic formula. The double bond equivalent (DBE) was calculated as fellows; $DBE = 1 + 0.5\,(2C - H + N + P)$. The Van Krevelen and DBE versus carbon number plots were produced according to the methods previously reported (Kew et al., 2017). The Venn plot of volatile compounds was analyzed via OriginPro2018.

2.7. Statistical analysis

The changing rates of physical and chemical factors were fitted into cubic polynomials via OriginPro2018. CCA and VPA were conducted based on fermentation parameters, the relative abundance of bacterial and fungal communities via vegan package in R (http://vegan.r-forge.r-project.org/). To analyze the relationships among microbial communities, we calculated all possible Spearman's rank correlations between the abundant genera (average relative abundance > 1%; majority >

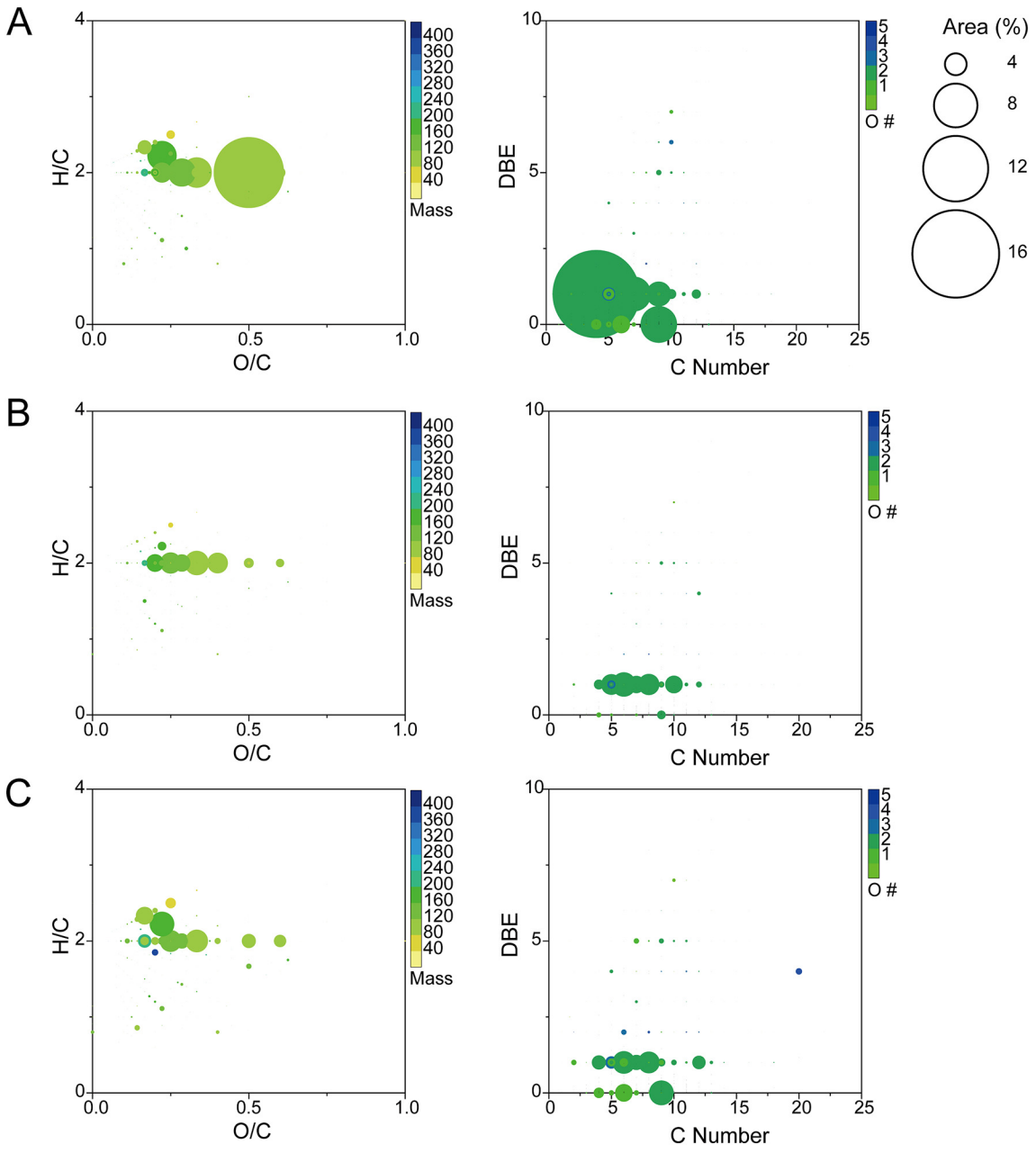

Fig. 1. Van Krevelen (left) and DBE versus carbon number plots (right) for three different base liquors; (top to bottom) (A) group S, (B) group T, (C) group F. In the van Krevelen diagrams, the coordinates of nodes depended on molecular formulas; the colors of nodes represented mass of formulas; the sizes of nodes were based on the peak areas. In the DBE versus carbon plots, points are colored according to oxygen number and sized according to peak areas.

50%). Only significant correlations ($p < 0.05$, with false discovery rate correction) were considered as valid correlations. Network was created by Gephi to sort through and visualize the correlations between microbiota (Bastian et al., 2009). All significance tests were calculated via SPSS (version 19.0).

2.8. Molecular ecological network analysis

The molecular ecological network analysis (MENA) was calculated via online tools (Deng et al., 2012; Zhou et al., 2010). The OTU table was used to construct the Random Matrix Theory (RMT)-based network (http://ieg2.ou.edu/MENA/main.cgi). The ecological networks were constructed with the following steps. First, we standardized the matrix of OTU table into the relative abundance for subsequent Pearson correlation analysis and network construction. Second, an appropriate threshold was calculated according to random matrix theory as filter for node associations. Third, we performed the module separation and modularity calculation according to topology properties of network. ZP-plot was conducted based on parameters of modularity analysis. The modularity analysis of network was applied to analyze the microbial interactions at OTU level and to evaluate network stability of each group (Y. Jiang et al., 2015; Olesen et al., 2007; Thebault and Fontaine, 2010).

2.9. SourceTracker analysis

To evaluate the enrichment of microbiota from pit mud, SourceTracker (v0.9.8) was used with the default parameters (Knights et al., 2011). Fermented grains samples of group S, T and F (4 day) were set as sink. Microbial community from *Daqu* and pit mud was set as sources.

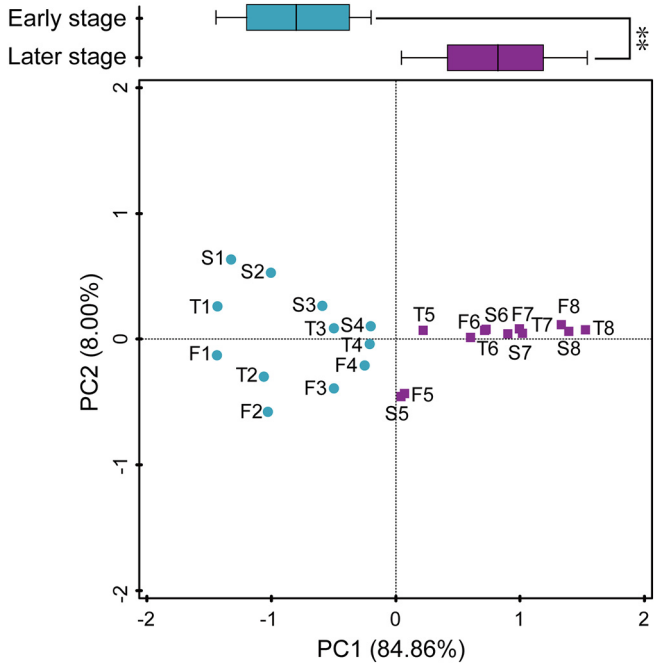

Fig. 2. Stages division according to principal components analysis (PCoA) based on Bray-Curtis dissimilarity matrix of fermentation parameters. Each circle represents the placement of endogenous factors of one sample; colors and shapes correspond to the stages in the top panel. Boxplots (top panel) indicate the distribution of each circle along the first principal coordinate (PC1). Boxplot center values represent the median and error bars represent the SD, significant test of the values of the two groups are carried ($p < 0.01$, by Mann-Whitney U test). Capital letters represent different groups. The numbers after the letters, in turn, represent the fermentation days of 4, 7, 9, 13, 19, 25, 31 and 40.

2.10. Accession number(s)

All sequences generated were submitted to the NCBI database under accession number PRJNA542688.

3. Results

3.1. Profiles of volatile metabolites in fermented grains and distillates

Fig. S2 and Dataset 1 show that 482, 550 and 563 volatile metabolites of group S (fermentation with sorghum), group T (fermentation with sorghum, wheat, corn) and group F (fermentation with sorghum, wheat, corn, rice and glutinous rice) were identified in base liquor, respectively. Group F contained 187 unique volatile metabolites, which accounted for 20.40% of total compounds. Group T contained 156 unique volatile metabolites, which accounted for 17.00% of total compounds. Group S contained 137 unique volatile metabolites, which accounted for 15.00% of total compounds. Group F and group T shared the most number of compounds between two groups. Dataset 1 and Fig. S2 show that three groups shared 245 volatile metabolites, which accounted for 26.80% of total compounds. Among them, 27 alcohols, 12 aldehydes, 11 organic acids and 97 esters were classified.

The chemical formulae and peak areas (%) of compounds were analyzed to generate van Krevelen and double bond equivalent (DBE) versus carbon number plots (Dataset 1). The van Krevelen plots show that all samples had large peak areas (%) for esters at H/C of 2, representing formulae including $C_4H_8O_2$ and $C_8H_{16}O_2$, compounds that may be formed during fermentation or distillation process. From the central position of O/C of 0 and H/C of 2, there are lines extending outwards in multiple directions. It reflected to the variety of alcohols, aldehydes, organic acids and esters, and indicated these compounds were abundant in all base liquors (Fig. 1).

The van Krevelen plot for group S shows a large area of ethyl acetate at H/C of 2 and O/C of 0.5 but not in group T and group F (Fig. 1A left, Fig. 1B left and C left). The group S had the largest standard deviation of compounds content (Dataset 1). It was worth noting that group F and group S contained less ratio of ethyl acetate but more ratio of ethyl hexanoate than that of group S. The diversity of aromatic and heterocyclic components was higher in group F compared with group S. In addition, some important flavor compounds were lacked in group S, such as 3-ethyl-2, 5-dimethylpyrazine (Dataset 1). Besides, the DBE versus carbon number plots (Fig. 1 right) show similar trends of volatile metabolites profile with that in the van Krevelen plots. All base liquors showed a variety of compounds with low DBE values, and the carbon number of compounds was ranging from 2 to 20. However, the DBE plot of group S was sparser due to the lower diversity of volatile metabolites than the other two groups. Furthermore, group F showed a higher ratio of medium and long chain compounds than S group (Fig. 1A right).

In addition, we checked the content of volatile metabolites in its corresponding fermented grains. It showed that the content of several important flavor compounds had a significant difference (Log_2 FC > 2) in fermented grains, such as ethyl octanoate, hexyl hexanoate and ethyl heptanoate (Dataset 2).

3.2. Dynamics of fermentation parameters during Baijiu making process

We found that both mixed cereals and single cereal fermentation existed two stages during fermentation. Fermentation of early stage showed significant ($p < 0.01$) difference compared with later stage on principal component 1 (PC1). Samples of S5 to S8, T5 to T8 and F5 to F8 formed a cluster in the later stage, while samples of S1 to S4, T1 to T4 and F1 to F4 formed another cluster in the early stage. Nevertheless, samples among three groups were more similar in the later stage than in the early stage (Fig. 2).

In order to expound the biological significance of clusters, we calculated the correlation between fermentation parameters with PC1 values. All fermentation parameters showed significantly correlation with PC1. Among them, starch and reducing sugar showed significantly negative correlation with PC1, whereas other fermentation parameters showed significantly positive correlation with PC1 (Fig. S3). Then we observed the changes of fermentation parameters through the whole fermentation process. It was showed that the utilization of starch and reducing sugar was faster in the early stage than later stage. During early stage, the content of starch decreased from 209.45 g/kg, 212.15 g/kg and 221.28 g/kg to 166.80 g/kg, 162.05 g/kg and 156.23 g/kg within 20 days in S, T and F group, but the utilization was halved within the next 20 days. Similar trends were also reflected in the content of reducing sugar between two stages. The metabolism of alcohol was quite rapid during the early stage, and it stayed around 4° after stage shift. Temperature showed a rapid rising trend in the early stage reaching for over 30 °C within 20 days, and then slowly fell down in the later stage. Through whole fermentation process of three groups, the acidity totally increased about 2° within 30 days, and stayed around 4° after 30 days of fermentation. Moisture of fermented grains increased slowly during the early stage, rising from about 55% to about 57% within 20 days. Nevertheless, it increased rapidly during the later stage, rising from about 58% to about 61% within 10 days (Fig. S4).

3.3. Microbial succession and driving factors in the Baijiu making process of single cereal and mixed cereals fermentation

We applied high-throughput sequencing to reveal the microbial community structures of *Daqu*, fermented grains and pit mud. After quality control, 810,199 high quality reads from V3-V4 region of 16S rRNA gene sequences, and 693,628 high quality reads from internal transcribed spacer (ITS) region were obtained from 24 fermented grains samples. Meanwhile, 440,271 high quality reads from V3-V4 region of 16S rRNA gene sequences, and 1,022,578 high quality reads from ITS

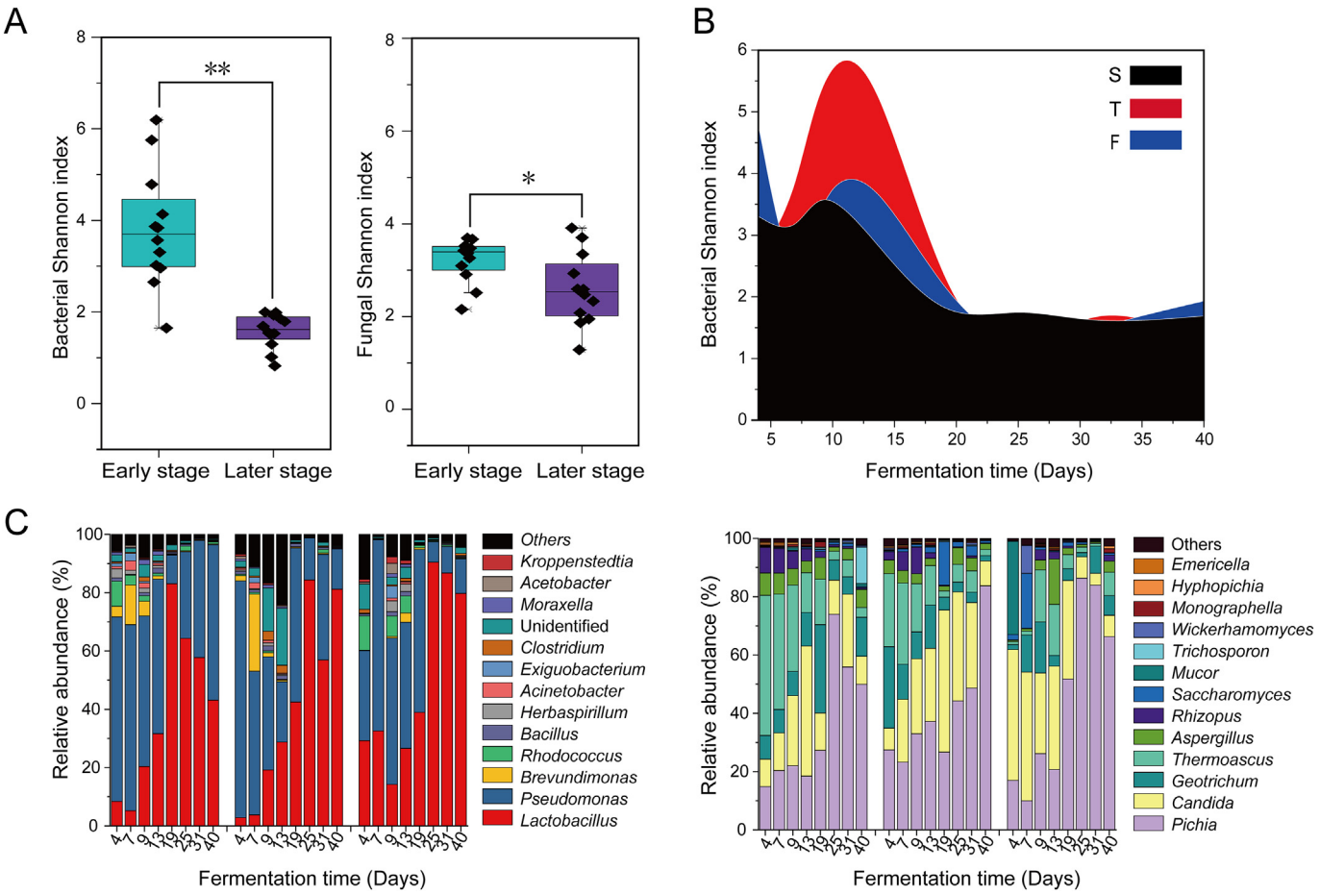

Fig. 3. Microbial diversity and succession of group S, T and F. (A) Box plots showing Shannon index values for bacterial (left) and fungal (right) communities between early stage and later stage ($^{*}p < 0.05$; $^{**}p < 0.01$; determined by one-way ANOVA test). (B) Density plot of bacterial Shannon index. (C) Bar plots of microbial structure at genus taxonomic level.

region were obtained from *Daqu* and pit mud samples. For bacteria, there was an average of 31,261 reads per sample, with a range from 19,123 to 63,477 reads. For fungi, there was an average of 42,905 reads per sample, with a range from 15,274 to 98,622 reads. Bacterial and fungal OTUs were clustered at a 97% similarity level of sequences. Then alpha diversity was calculated (Dataset 3).

We found that the microbial diversity was significantly ($p < 0.05$) higher during the early stage than the later stage according to Shannon index (Fig. 3A). For all groups, bacterial Shannon index rapidly decreased below two within 10 days before stage shifts. Nevertheless, the decline rate of bacterial diversity was different among the three groups. Compared with group S, group F and group T showed about 5 days delay of bacterial decline. Mixed cereals fermentation possessed longer time for maintaining high diversity of bacteria (Fig. 3B). Then we analyzed the bacterial structure of the three groups to furtherly understand the difference of bacterial succession rate. It was showed that the largest groups of bacterial genera were *Lactobacillus*, *Pseudomonas*, *Rhodococcus and Bacillus*. The genus *Lactobacillus* was the most abundant bacterial genus weather in group S, group T or F group, whose relative abundance could reach over 80% during the later stage (Fig. 3C left). The decrease of bacterial Shannon index showed the significant negative correlation ($p < 0.001$) with the growth of *Lactobacillus* (Table S1). Notably, *Lactobacillus* became the dominate genus of group S at the end of the early stage. For fungi, *Pichia*, *Candida*, *Thermomyces*, *Geotrichum* were the dominance of fungal genera. In the early stage, *Candida* were more abundant in group F than group S and group T. Besides, *Pichia* were more abundant in group F than group S and group T (Fig. 3C right).

Then we performed canonical correspondence analysis (CCA) and correlation analysis to clarify the relationship between microbial succession and fermentation stages. According to CCA results, the two axes explained 35.29%, 41.45% and 40.07% of the total variance in microbial community differentiation in group S, group T and group F, suggesting the remarkable correlations between microbial communities and fermentation parameters. However, different fermentation parameters led to distinct microbial succession rate (Fig. 4A). Group S showed the faster microbial succession rate due to significant ($p < 0.05$) correlations with fermentation parameters (Fig. 4B). Acidity and temperature were the key factors driving changes of bacterial diversity in the group S, whereas moisture was the key driving factor in the group T. As for fungi, the moisture, acidity and alcohol showed significant ($p < 0.05$) negative correlations with fungal Shannon index. Notably, the driving force of these fermentation parameters was not significant in group F (Fig. 4).

In order to clarify the specific species that led to the difference in the driving forces or influenced by driving factors, we analyzed the relationships between them in each group via Pearson's coefficient (Table S2). For group S, 21 OTUs showed significant ($p < 0.05$) negative correlation with acidity. Meanwhile, we found that some OTUs belong to *Lactobacillus* significantly ($p < 0.05$) correlated with temperature. For group T, 54 OTUs displayed significant ($p < 0.05$) correlation with fermentation parameters. Particularly, group F showed 74 OTUs had significant ($p < 0.05$) positive or negative correlation with fermentation parameters.

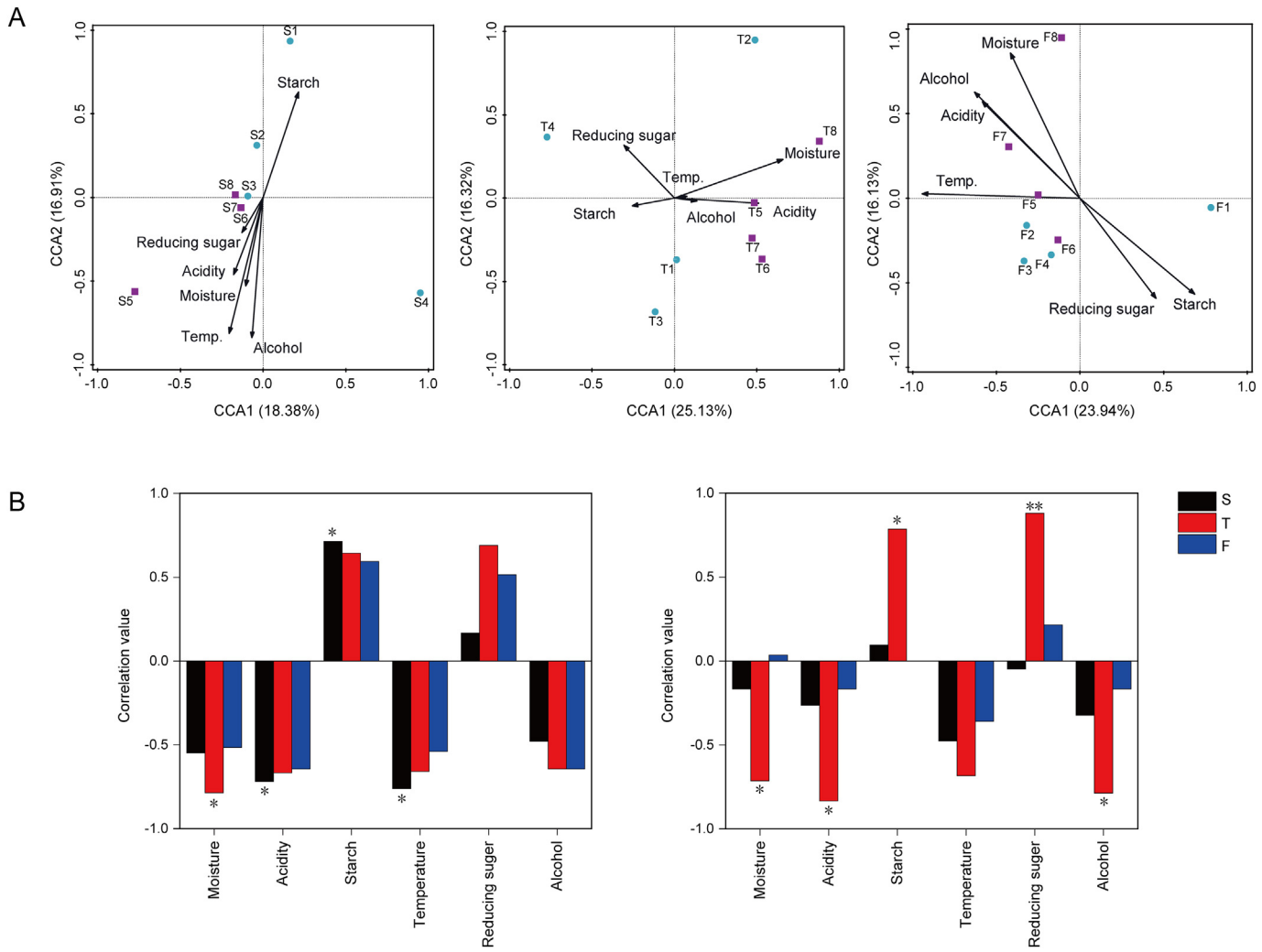

Fig. 4. Relationship between microbial succession and fermentation parameters. (A) Canonical correspondence analysis (CCA) of microbial community composition and fermentation parameters. Capital letters represent different groups. The numbers after the letters, in turn, represent the fermentation days of 4, 7, 9, 13, 19, 25, 31 and 40. The arrows indicate correlations between microbial community and fermentation parameters. (B) Bar plots of correlation between fermentation parameters with bacterial Shannon index (left) and fungal Shannon index (right); $^{*}p < 0.05$; $^{**}p < 0.01$, determined by one-way ANOVA test.

3.4. Microbial interaction and community stability in the single cereal and mixed cereals fermentation

We conducted network analysis to evaluate interactions among abundant microbiota at genus taxonomic level in each group. As the relationship showed in the Fig. S5, the significant ($p < 0.05$) negative coefficient of genera in group F was less than that in the other two groups. *Lactobacillus* displayed negative correlations between *Bacillus*, *Torulaspora* and *Aspergilllus* in group S, but not in group F and group T.

For comprehend the significance of microbial succession rate in the community-level, we conducted the molecular ecological network analysis (MENA) in each group. The results indicated that group F contained more OTUs with $Z_i > 2.5$ or $P_i > 0.6$, suggesting more network hubs and closer connection of network modules (Fig. 5). Group F had six OTUs with $P_i > 0.6$. Group T had five OTUs with $P_i > 0.6$. Group S had two OTUs with $P_i > 0.6$. For the Z_i values, group S also showed the least numbers of OTUs with $Z_i > 2.5$, whereas group F showed the most numbers of OTUs with $Z_i > 2.5$ among three groups.

3.5. Comparison of initial microbial enrichments during fermentation process

For further understand the initial difference in the early stage (Fig. 2), we collected pit mud and *Daqu* to compare microbial enrichment among the three groups. We used SourceTracker to predict the enrichment of microbes found in fermented grains. It was found that most of bacteria came from pit mud and most of fungi came from *Daqu* (Fig. 6). Source tracking results revealed that the pit mud contributed 24.47%, 11.69% and 56.51% of bacteria in group S, group T and group F, respectively. For all fermented grains, Clostridiales was the main enriched bacterial order from pit mud, and group F enriched the most ratio of that among three groups (Table S3).

4. Discussion

Different selection of cereals and starters significantly affects microbial succession and flavor profile of strong-aroma *Baijiu* fermentation (He et al., 2019; Jin et al., 2017; Shi et al., 2011). Frequently, base liquors produced in different batches have similar yield but different quality in strong-aroma *Baijiu* making process according to empirical practice. Previous research has illustrated the typical flavor profile of single cereal fermentation and mix cereals fermentation (Fan and Qian, 2006), but key factors regulating the flavor profile during the fermentation process remain unclear. Spontaneous food fermentation can hardly be controlled without understanding the relationship between metabolites and microbial community in a dynamic perspective. In this

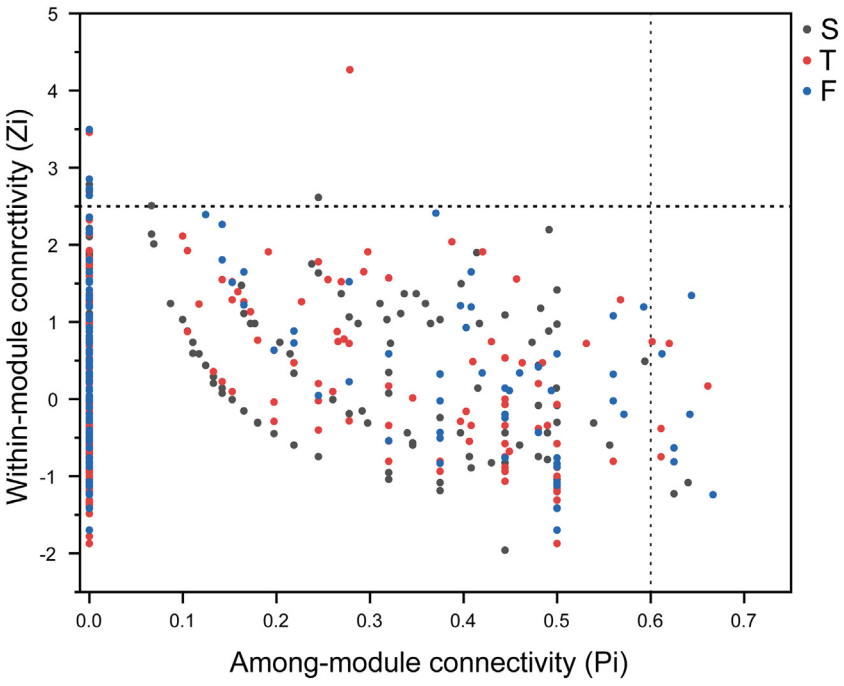

Fig. 5. ZP-plot showing distribution of OTUs based on their module-based topological roles. Each dot represents an OTU in the dataset of group S (black), group T (red) and group F (blue). The topological role of each OTU was determined according to the scatter plot of within-module connectivity (Zi) and among-module connectivity (Pi). (For interpretation of the references to colour in this figure legend, the reader is referred to the web version of this article.)

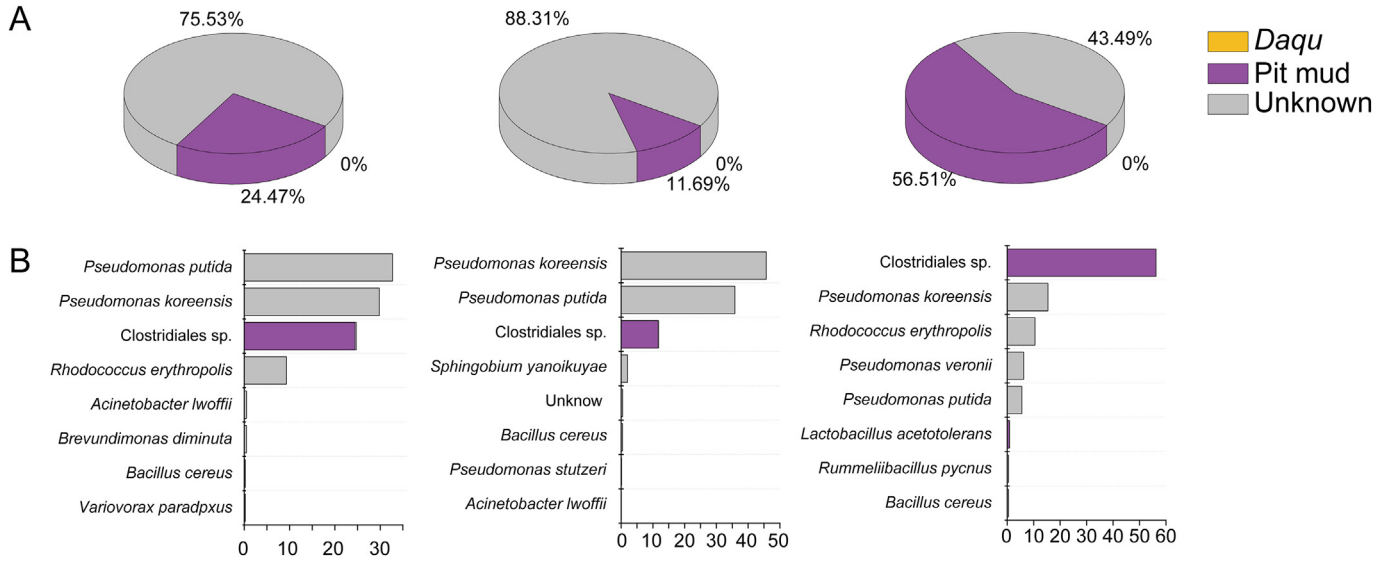

Fig. 6. SourceTracker results highlight the differences in enrichment ability of microbiota from pit mud. (A) Average percent contribution of specific source communities. (B) Source tracking analysis of bacterial communities for group S, T and F.

study, we explored a factor, named microbial succession rate, which contributed to the fermentation difference between single cereal fermentation and mixed cereal fermentation. We confirm that microbial succession rate is an enlightening view in solid-state fermentation.

Our results showed that all base liquors showed a variety of compounds with low DBE values and low carbon number of compounds compared with western liquors (Fig. 1). It reflected the typical traits of strong-aroma *Baijiu* (Fang et al., 2019; Kew et al., 2017). The various alcohols, aldehydes, organic acids and esters were the abundant volatile metabolites in *Baijius* (Fig. 1 and Dataset 1). Fermentation with mixed cereals increased the diversity of volatile metabolites (Fig. S2). Similar with previous studies (Fan and Qian, 2006; Yao et al., 2015), the mixed cereal fermentation showed high diversity of aromatic and heterocyclic components (Dataset 1). In addition, it was suggested that most non-volatile organic compounds of *Baijiu* were organic acid and polyhydric alcohol (Fang et al., 2019). Thus, we determined the acidity, reducing sugar, alcohol, moisture and starch as a rough profile of metabolites during fermentation. Besides, because of the importance of bio-heat (Xiao et al., 2017), we also monitored the temperature during the process of fermentation.

In the process of strong-aroma *Baijiu* fermentation, we found that the fermentation parameters marked the process with two stages (Fig. 2). During the early stage, the alcohol content and temperature increased rapidly, whereas the content of starch and reducing sugar decreased rapidly. It implied the flourishing growth of the microbial community with a lot of bio-heat produced (Xiao et al., 2017). During the later stage, the acidity and moisture displayed a fast upward trend, suggesting these two factors could drive the stage shift of fermentation (Fig. S4). Our results suggested that fermentation stages not only existed in the process of light-aroma and soy sauce-aroma *Baijiu*, but also in the process of strong-aroma *Baijiu* (Song et al., 2017; Wang et al., 2019).

Evidently, microorganisms play critical roles in the characteristics of the flavor metabolites across stages (Jin et al., 2017; Nie et al., 2017; Song et al., 2017). In order to explain the difference of metabolic profile between single cereal fermentation and mixed cereals fermentation, we analyzed the link between microbial community and fermentation parameters in each group. Compared with previous studies (Wang et al., 2019; Wang et al., 2018), the total variance explanations of CCA displayed a remarkable correlations between microbial communities and fermentation parameters in each group (Fig. 4A). Traditionally, fermentation parameters distinctly reflected microbial succession in the fermentation microbiota (Song et al., 2017). However, correlation analysis indicated that the driving force of each fermentation factor was not significantly associated with microbial diversity in group F (Fig. 4B), suggesting the microbial succession rate could be the important factor that regulated the metabolic difference.

In the process of *Baijiu* making, *Lactobacillus* was the dominant genus in later stage of fermentation, and the rapid increase of its relative abundance implied the stage shift of fermentation. (Jin et al., 2017; Song et al., 2017; Wang et al., 2019; Wang et al., 2018). Therefore, we found that *Lactobacillus* could be a biomarker for description of microbial succession rate in strong-aroma *Baijiu* fermentation (Fig. 3C and Table S1).

Previous studies also suggested that diverse metabolites were often associated with complex microbial interactions (Liu et al., 2017; Wang et al., 2019), whereas microbial interactions were associated with microbial succession and diversity (Layeghifard et al., 2017). The different microbial succession rate implied that mixed cereals fermentation might benefit the microbial diversity, and had an impact on microbial interactions. From a network perspective, we found that mixed cereals fermentation showed less number of significant negative correlations than single cereal fermentation. Notably, *Bacillus* showed significant negative correlation with other genera in group S (Fig. S5). Previous studies claimed that *Bacillus* was associated with the metabolism of pyrazinones and dihydropyrazinones (Guo et al., 2017). Thus, it could explain why less dihydropyrazinones were detected in group S. Furthermore, the network of mixed cereals fermentation contained more OTUs across and within modules than that of single cereal fermentation, suggesting more hubs exist in network (Fig. 5). It means more complex coexistence relationship and higher stability of microbial community (Deng et al., 2012; Y.J. Jiang et al., 2015; Layeghifard et al., 2017; Tong et al., 2019). Therefore, mixed cereals fermentation showed slower microbial succession rate than single cereal fermentation, and produced diverse metabolites.

Moreover, it was convinced that microbial fitness and fraction of immigrants could affect the microbial succession (Cira et al., 2018), thus, we conducted source tacking to observe the microbial immigrants in each group. Fermentation with sorghum, wheat, corn, rice and glutinous rice was conducive to improving the ability of enriching Clostridiales from pit mud (Fig. 6), which could be a potential positive influence on flavor (Chai et al., 2019; Hu et al., 2016; Weimer et al., 2015). Although it remains unclear how cereals promote the microbial immigrants, we surmise it might depend on nutritional acquisition availability of the microorganisms, since mixed cereals fermentation showed higher reducing sugar and lower acidity than single cereal fermentation (Alijosius et al., 2016; Goldford et al., 2018; Poutanen et al., 2009).

In general, we conclude that microbial succession rate caused flavor difference in strong-aroma *Baijiu* making process. The microbial succession rate mainly reflected in two periods: the initial stage of microbial enrichment and the stage shift period with microbial diversity decline. Slower stage shift rate and faster fermentation start-up rate benefitted the microbial enrichment and diversity maintenance. In addition, fermentation parameters drove the different microbial succession rate, which might originate from the initial difference caused by raw materials. Our work addressed the microbial succession rate, a dynamic perspective of solid-state fermentation, in the system of strong-aroma *Baijiu* making process.

Supplementary data to this article can be found online at https://doi.org/10.1016/j.ijfoodmicro.2019.108350.

Declaration of competing interest

The authors declare that they have no known competing financial interests or personal relationships that could have appeared to influence the work reported in this paper.

Acknowledgements

This work was supported by the National Natural Science Foundation of China (NSFC) (grants 31530055), National Key Research and Development Program of China (2018YFC1604100), National First-class Discipline Program of Light Industry Technology and Engineering (LITE2018-12), the Key Laboratory of Wuliangye-flavor Liquor Solid-state Fermentation, China National Light Industry (2017JJ017), the Program of Introducing Talents of Discipline to Universities (111 Project) (grant 111-2-06), and Postgraduate Research & Practice Innovation Program of Jiangnan University (grant JNKY19_014).

References

Ai, M., Qiu, X., Huang, J., We, C., Jin, Y., Zhou, R., 2019. Characterizing the microbial diversity and major metabolites of Sichuan bran vinegar augmented by Monascus purpureus. Int. J. Food Microbiol. 292, 83–90.

Alijosius, S., Svirmickas, G.J., Bliznikas, S., Gruzauskas, R., Sasyte, V., Raceviciute-Stupeliene, A., Kliseviciute, V., Dauksienr, A., 2016. Grain chemical composition of different varieties of winter cereals. Zemdirbyste-Agriculture 103, 273–280.

Bastian, M., Heymann, S., Jacomy, M., 2009. Gephi: an open source software for exploring and manipulating networks. ICWSM 8, 361–362.

Bokulich, N.A., Collins, T.S., Masarweh, C., Allen, G., Heymann, H., Ebeler, S.E., Mills, D. A., 2016. Associations among wine grape microbiome, metabolome, and fermentation behavior suggest microbial contribution to regional wine characteristics. mBio 7, e00631–16.

Bolger, A.M., Lohse, M., Usadel, B., 2014. Trimmomatic: a flexible trimmer for Illumina sequence data. Bioinformatics 30, 2114–2120.

Bravo, L., Siddhuraju, P., Saura-Calixto, F., 1998. Effect of various processing methods on the in vitro starch digestibility and resistant starch content of Indian pulses. J. Agric. Food Chem. 46, 4667–4674.

Caporaso, J.G., Kuczynski, J., Stombaugh, J., Bittinger, K., Bushman, F.D., Costello, E.K., Fierer, N., Pena, A.G., Goodrich, J.K., Gordon, J.I., 2010. QIIME allows analysis of high-throughput community sequencing data. Nat. Methods 7, 335–336.

Chai, L.-J., Xu, P.-X., Qian, W., Zhang, X.-J., Ma, J., Lu, Z.-M., Wang, S.-T., Shen, C.-H., Shi, J.-S., Xu, Z.-H., 2019. Profiling the Clostridia with butyrate-producing potential in the mud of Chinese liquor fermentation cellar. Int. J. Food Microbiol. 297, 41–50.

Cira, N.J., Pearce, M.T., Quake, S.R., 2018. Neutral and selective dynamics in a synthetic microbial community. Proc. Natl. Acad. Sci. U. S. A. 115, E9842–E9848.

Datta, M.S., Sliwerska, E., Gore, J., Polz, M.F., Cordero, O.X., 2016. Microbial interactions lead to rapid micro-scale successions on model marine particles. Nat. Commun. 7, 11965.

Deng, Y., Jiang, Y.-H., Yang, Y., He, Z., Luo, F., Zhou, J., 2012. Molecular ecological network analyses. BMC Bioinf. 13, 113.

Du, H., Wang, X., Zhang, Y., Xu, Y., 2019. Exploring the impacts of raw materials and environments on the microbiota in Chinese Daqu starter. Int. J. Food Microbiol. 297, 32–40.

Dunkel, A., Steinhaus, M., Kotthoff, M., Nowak, B., Krautwurst, D., Schieberle, P., Hofmann, T., 2014. Nature's chemical signatures in human olfaction: a foodborne perspective for future biotechnology. Angew. Chem. Int. Ed. 53, 7124–7143.

Edgar, R.C., Haas, B.J., Clemente, J.C., Quince, C., Knight, R., 2011. UCHIME improves sensitivity and speed of chimera detection. Bioinformatics 27, 2194–2200.

Fan, W.L., Qian, M.C., 2006. Characterization of aroma compounds of Chinese "Wuliangye" and "Jiannanchun" liquors by aroma extract dilution analysis. J. Agric. Food Chem. 54, 2695–2704.

Fang, C., Du, H., Jia, W., Xu, Y., 2019. Compositional differences and similarities between typical Chinese baijiu and Western liquor as revealed by mass spectrometry-based metabolomics. Metabolites 9, 2.

Gao, W., Fan, W., Xu, Y., 2014. Characterization of the key odorants in light aroma type Chinese liquor by gas chromatography–olfactometry, quantitative measurements, aroma recombination, and omission studies. J. Agric. Food Chem. 62, 5796–5804.

Goldford, J.E., Lu, N., Bajic, D., Estrela, S., Tikhonov, M., Sanchez-Gorostiaga, A., Segre, D., Mehta, P., Sanchez, A., 2018. Emergent simplicity in microbial community assembly. Science 361, 469–474.

Grainger, T.N., Letten, A.D., Gilbert, B., Fukami, T., 2019. Applying modern coexistence theory to priority effects. Proc. Natl. Acad. Sci. U. S. A. 116, 6205–6210.

Guo, C.J., Chang, F.Y., Wyche, T.P., Backus, K.M., Acker, T.M., Funabashi, M., Taketani, M., Donia, M.S., Nayfach, S., Pollard, K.S., Craik, C.S., Cravatt, B.F., Clardy, J., Voigt,

C.A., Fischbach, M.A., 2017. Discovery of reactive microbiota-derived metabolites that inhibit host proteases. Cell 168, 517–526.
He, G., Huang, J., Zhou, R., Wu, C., Jin, Y., 2019. Effect of fortified daqu on the microbial community and flavor in Chinese strong-flavor liquor brewing process. Front. Microbiol. 10, 56.
Hu, X., Du, H., Ren, C., Xu, Y., 2016. Illuminating anaerobic microbial community and cooccurrence patterns across a quality gradient in Chinese liquor fermentation pit muds. Appl. Environ. Microbiol. 82, 2506–2515.
Jiang, Y., Sun, B., Li, H., Liu, M., Chen, L., Zhou, S., 2015. Aggregate-related changes in network patterns of nematodes and ammonia oxidizers in an acidic soil. Soil Biol. Biochem. 88, 101–109.
Jiang, Y.J., Sun, B., Li, H.X., Liu, M.Q., Chen, L.J., Zhou, S., 2015. Aggregate-related changes in network patterns of nematodes and ammonia oxidizers in an acidic soil. Soil Biol. Biochem. 88, 101–109.
Jiang, Z.M., Chen, Y., Wang, D.L., Wang, X.L., Shang, K., Zhang, S., Li, Y.Y., 2016. The influence of porosity of the grain medium on the flavour formation of Chinese liquor during solid-state fermentation. J. Inst. Brew. 122, 468–472.
Jin, G., Zhu, Y., Xu, Y., 2017. Mystery behind Chinese liquor fermentation. Trends Food Sci. Technol. 63, 18–28.
Kew, W., Goodall, I., Clarke, D., Uhrin, D., 2017. Chemical diversity and complexity of scotch whisky as revealed by high-resolution mass spectrometry. J. Am. Soc. Mass Spectrom. 28, 200–213.
Knights, D., Kuczynski, J., Charlson, E.S., Zaneveld, J., Mozer, M.C., Collman, R.G., Bushman, F.D., Knight, R., Kelley, S.T., 2011. Bayesian community-wide culture-independent microbial source tracking. Nat. Methods 8, 761–U107.
Kõljalg, U., Nilsson, R.H., Abarenkov, K., Tedersoo, L., Taylor, A.F.S., Bahram, M., Bates, S.T., Bruns, T.D., Bengtsson-Palme, J., Callaghan, T.M., Douglas, B., Drenkhan, T., Eberhardt, U., Dueñas, M., Grebenc, T., Griffith, G.W., Hartmann, M., Kirk, P.M., Kohout, P., Larsson, E., Lindahl, B.D., Lücking, R., Martín, M.P., Matheny, P.B., Nguyen, N.H., Niskanen, T., Oja, J., Peay, K.G., Peintner, U., Peterson, M., Põldmaa, K., Saag, L., Saar, I., Schüßler, A., Scott, J.A., Senés, C., Smith, M.E., Suija, A., Taylor, D.L., Telleria, M.T., Weiss, M., Larsson, K.-H., 2013. Towards a unified paradigm for sequence-based identification of fungi. Mol. Ecol. 22, 5271–5277.
Layeghifard, M., Hwang, D.M., Guttman, D.S., 2017. Disentangling interactions in the microbiome: a network perspective. Trends Microbiol. 25, 217–228.
Liu, H., Sun, B., 2018. Effect of fermentation processing on the flavor of baijiu. J. Agric. Food Chem. 66, 5425–5432.
Liu, Y., Rousseaux, S., Tourdot-Marechal, R., Sadoudi, M., Gougeon, R., Schmitt-Kopplin, P., Alexandre, H., 2017. Wine microbiome: a dynamic world of microbial interactions. Crit. Rev. Food Sci. Nutr. 57, 856–873.
Lu, Z.-M., Wang, Z.-M., Zhang, X.-J., Mao, J., Shi, J.-S., Xu, Z.-H., 2018. Microbial ecology of cereal vinegar fermentation: insights for driving the ecosystem function. Curr. Opin. Biotechnol. 49, 88–93.
McAuliffe, O., Kilcawley, K., Stefanovic, E., 2019. Symposium review: genomic investigations of flavor formation by dairy microbiota. J. Dairy Sci. 102, 909–922.
Miller, G.L., 1959. Use of dinitrosalicylic acid reagent for determination of reducing sugar. Anal. Chem. 31, 426–428.
Nie, Z., Zheng, Y., Xie, S., Zhang, X., Song, J., Xia, M., Wang, M., 2017. Unraveling the correlation between microbiota succession and metabolite changes in traditional Shanxi aged vinegar. Sci. Rep. 7, 9240.
Olesen, J.M., Bascompte, J., Dupont, Y.L., Jordano, P., 2007. The modularity of pollination networks. Proc. Natl. Acad. Sci. U. S. A. 104, 19891–19896.
Poutanen, K., Flander, L., Katina, K., 2009. Sourdough and cereal fermentation in a nutritional perspective. Food Microbiol. 26, 693–699.
Shi, S., Zhang, L., Wu, Z.Y., Zhang, W.X., Deng, Y., Zhong, F.D., Li, J.M., 2011. Analysis of the fungi community in multiple- and single-grains Zaopei from a Luzhou-flavor liquor distillery in western China. World J. Microbiol. Biotechnol. 27, 1869–1874.
Song, Z., Du, H., Zhang, Y., Xu, Y., 2017. Unraveling core functional microbiota in traditional solid-state fermentation by high-throughput amplicons and metatranscriptomics sequencing. Front. Microbiol. 8, 1294.
Thebault, E., Fontaine, C., 2010. Stability of ecological communities and the architecture of mutualistic and trophic networks. Science 329, 853–856.
Tong, X., Leung, M.H.Y., Wilkins, D., Cheung, H.H.L., Lee, P.K.H., 2019. Neutral processes drive seasonal assembly of the skin mycobiome. mSystems 4, e00004–e00019.
Wang, X., Du, H., Zhang, Y., Xu, Y., 2018. Environmental microbiota drives microbial succession and metabolic profiles during Chinese liquor fermentation. Appl. Environ. Microbiol. 84, e02369–02317.
Wang, S., Wu, Q., Nie, Y., Wu, J., Xu, Y., 2019. Construction of synthetic microbiota for reproducible flavor metabolism in Chinese light aroma type liquor produced by solid-state fermentation. Appl. Environ. Microbiol. 10, e03090–03018.
Weimer, P.J., Nerdahl, M., Brandl, D.J., 2015. Production of medium-chain volatile fatty acids by mixed ruminal microorganisms is enhanced by ethanol in co-culture with Clostridium kluyveri. Bioresour. Technol. 175, 97–101.
Wu, Q., Cao, S., Xu, Y., 2017. Effects of glutinous and nonglutinous sorghums on Saccharomyces cerevisiae fermentation for Chinese liquor making. Int. J. Food Sci. Technol. 52, 1348–1357.
Xiao, C., Lu, Z.-M., Zhang, X.-J., Wang, S.-T., Ao, L., Shen, C.-H., Shi, J.-S., Xu, Z.-H., 2017. Bio-heat is a key environmental driver shaping the microbial community of medium-temperature daqu. Appl. Environ. Microbiol. 83, e01550–01517.
Yao, F., Yi, B., Shen, C., Tao, F., Liu, Y., Lin, Z., Xu, P., 2015. Chemical analysis of the Chinese liquor Luzhoulaojiao by comprehensive two-dimensional gas chromatography/time-of-flight mass spectrometry. Sci. Rep. 5, 9553.
Zhang, J., Guo, Z., Xue, Z., Sun, Z., Zhang, M., Wang, L., Wang, G., Wang, F., Xu, J., Cao, H., Xu, H., Lv, Q., Zhong, Z., Chen, Y., Qimuge, S., Menghe, B., Zheng, Y., Zhao, L., Chen, W., Zhang, H., 2015. A phylo-functional core of gut microbiota in healthy young Chinese cohorts across lifestyles, geography and ethnicities. ISME J. 9, 1979–1990.
Zhou, J., Deng, Y., Luo, F., He, Z., Tu, Q., Zhi, X., 2010. Functional molecular ecological networks. mBio 1, e00169–00110.